Supplement of Geosci. Model Dev., 13, 3731–3768, 2020
https://doi.org/10.5194/gmd-13-3731-2020-supplement

Geoscientific Model Development
Open Access

Supplement of

Global aerosol simulations using NICAM.16 on a 14 km grid spacing for a climate study: improved and remaining issues relative to a lower-resolution model

Daisuke Goto et al.

Correspondence to: Daisuke Goto (goto.daisuke@nies.go.jp)

Table S1: Observation sites of AOT.

Site	Country	Network[#1]	LON	LAT
BONDVILLE	US	A	-88.37	40.05
BSRN_BAO_Boulder	US	A	-105.01	40.05
Billerica	US	A	-71.27	42.53
Bozeman	US	A	-111.05	45.66
Bratts_Lake	US	A	-104.70	50.28
CARTEL	US	A	-71.93	45.38
Cart_Site	US	A	-97.49	36.61
Egbert	US	A	-79.75	44.23
Fresno	US	A	-119.77	36.78
GSFC	US	A	-76.84	38.99
HJAndrews	US	A	-122.22	44.24
Halifax	US	A	-63.59	44.64
KONZA_EDC	US	A	-96.61	39.10
Kangerlussuaq	US	A	-50.62	67.00
La_Parguera	US	A	-67.05	17.97
MD_Science_Center	US	A	-76.62	39.28
Mauna_Loa	US	A	-155.58	19.54
Mexico_City	US	A	-99.18	19.33
Missoula	US	A	-114.08	46.92
Pickle_Lake	US	A	-90.22	51.45
Railroad_Valley	US	A	-115.96	38.50
Rimrock	US	A	-116.99	46.49
Rogers_Dry_Lake	US	A	-117.89	34.93
SERC	US	A	-76.50	38.88
Saturn_Island	US	A	-123.13	48.78
Sevilleta	US	A	-106.89	34.36
Sioux_Falls	US	A	-96.63	43.74
TABLE_MOUNTAIN_CA	US	A	-117.68	34.38
Alta_Floresta	Brazil	A	-56.10	-9.87
Arica	Chile	A	-70.31	-18.47
CEILAP-BA	Argentina	A	-58.50	-34.57
CUIABA-MIRANDA	Brazil	A	-56.02	-15.73
Campo_Grande_SONDA	Brazil	A	-54.54	-20.44
Trelew	Argentina	A	-65.31	-43.25
ATHENS-NOA	Greece	A	23.78	37.99
Autilla	Spain	A	-4.60	42.00
Belsk	Poland	A	20.79	51.84
Blida	Algeria	A	2.88	36.51
Bucharest_Inoe	Romania	A	26.03	44.35
Burjassot	Spain	A	-0.42	39.51
Carpentras	France	A	5.06	44.08
El_Arenosillo	Spain	A	-6.73	37.11
Ersa	France	A	9.36	43.00
Evora	Portugal	A	-7.91	38.57
FORTH_CRETE	Greece	A	25.28	35.33

Granada	Spain	A	-3.61	37.16
Gustav_Dalen_Tower	Swedish coast	A	17.47	58.59
IMS-METU-ERDEMLI	Turkey	A	34.26	36.57
Ispra	Italy	A	8.63	45.80
Kyiv	Ukraine	A	30.50	50.36
Lampedusa	Italy	A	12.63	35.52
Lecce_University	Italy	A	18.11	40.34
Lille	France	A	3.14	50.61
Malaga	Spain	A	-4.48	36.72
Minsk	Belarus	A	27.60	53.92
Modena	Italy	A	10.95	44.63
Moldova	Moldova	A	28.82	47.00
Moscow_MSU_MO	Russia	A	37.51	55.70
OHP_OBSERVATOIRE	France	A	5.71	43.94
Palaiseau	France	A	2.21	48.70
Palencia	Spain	A	-4.52	41.99
Rome_Tor_Vergata	Italy	A	12.65	41.84
Sevastopol	Ukraine	A	33.52	44.62
Thessaloniki	Greece	A	22.96	40.63
Toravere	Estonia	A	26.46	58.26
Toulon	France	A	6.01	43.14
Capo_Verde	Sal Island	A	-22.94	16.73
Dakar	Senegal	A	-16.96	14.39
Dhadnah	UAE	A	56.33	25.51
Eilat	Israel	A	34.92	29.50
IER_Cinzana	Mali	A	-5.93	13.28
Ilorin	Nigeria	A	4.34	8.32
Izana	Spain	A	-16.50	28.31
Nes_Ziona	Israel	A	34.79	31.92
SEDE_BOKER	Israel	A	34.78	30.86
Santa_Cruz_Tenerife	Tenerife	A	-16.25	28.47
Solar_Village	Saudi Arabia	A	46.40	24.91
Mongu	Zambia	A	23.15	-15.25
REUNION_ST_DENIS	France	A	55.48	-20.88
Skukuza	South Africa	A	31.59	-24.99
Birdsville	Australia	A	139.35	-25.90
Canberra	Australia	A	149.11	-35.27
Jabiru	Australia	A	132.89	-12.66
Lake_Argyle	Australia	A	128.75	-16.11
Lauder	New Zealand	S	169.68	-45.04
Chiang_Mai_Met_Sta	Thailand	A	98.97	18.77
Dushanbe	Tajikistan	A	68.86	38.55
Kanpur	India	A	80.23	26.51
Karachi	Pakistan	A	67.03	24.87
Shirahama	Japan	A	135.36	33.69
Silpakorn_Univ	Thailand	A	100.04	13.82
Yakutsk	Russia	A	129.37	61.66
Sendai	Japan	S	140.84	38.26

Chiba	Japan	S	140.10	35.63
Hedo	Japan	S	128.25	26.87
Miyako	Japan	S	125.33	24.74
SACOL	China	A	104.14	35.95
XiangHe	China	A	116.96	39.75
Akedala	China	C	87.97	47.12
Lhasa	China	C	91.13	29.67
Mt.Waliguan	China	C	100.92	36.28
Shangri-La	China	C	99.73	28.02
Dunhuang	China	C	94.68	40.15
Ejina	China	C	101.07	41.95
Hami	China	C	93.52	42.82
Hotan	China	C	79.93	37.13
Jiuquan	China	C	98.48	39.77
Minqin	China	C	103.08	38.63
Tazhong	China	C	83.67	39.00
Urumqi	China	C	108.52	41.57
Xilinhot	China	C	116.12	43.95
Zhangbei	China	C	114.70	41.15
Zhurihe	China	C	112.90	42.40
Dongsheng	China	C	109.98	39.83
Mt.Caolan	China	C	103.85	36.00
Yan'an	China	C	109.50	36.60
Yulin	China	C	109.20	38.43
Changde	China	C	111.70	29.17
Dongtan	China	C	121.96	31.52
Gucheng	China	C	115.80	39.13
Huimin	China	C	117.53	37.48
Lin'an	China	C	119.73	30.30
Mt.Longfeng	China	C	127.60	44.73
Mt.Tai	China	C	117.10	36.25
Shangdianzi	China	C	117.12	40.65
Tongyu	China	C	122.87	44.42
Yushe	China	C	112.98	37.07
Anshan	China	C	123.00	41.08
Beijing	China	C	116.47	39.80
Benxi	China	C	123.78	41.32
Chengdu	China	C	104.03	30.65
Dalian	China	C	121.63	38.90
Datong	China	C	113.33	40.10
Fushun	China	C	123.95	41.88
Hangzhou	China	C	120.17	30.23
Hefei	China	C	116.38	31.98
Kuming	China	C	102.65	25.01
Lanzhou	China	C	103.88	36.05
Naning	China	C	118.77	32.05
Nanjing	China	C	108.35	22.82
Panyu	China	C	113.35	23.00

Pudong	China	C	121.55	31.22
Shenyang	China	C	123.50	41.77
Tianjin	China	C	117.17	39.10
Wulate	China	C	87.62	43.78
Xi'an	China	C	108.97	34.43
Yinchuan	China	C	106.22	38.48
Zhengzhou	China	C	113.68	34.78

#1 The network includes A (AERONET), S (SKYNET) and C (CARINET).

Table S2: Observation sites of BC, POM and sulfate mass concentrations at the surface.

Code	Site	Country	Network[#1]	LON	LAT	BC	POM	Sulfate
ACAD1	Acadia NP	US	I	-68.26	44.38	○	○	○
ADPI1	Addison Pinnacle	US	I	-77.21	42.09	○	○	○
AGTI1	Agua Tibia	US	I	-116.97	33.46	○	○	○
AREN1	Arendtsville	US	I	-77.31	39.92	○	○	○
ATLA1	South Dekalb	US	I	-84.29	33.69	○	○	○
BADL1	Badlands NP	US	I	-101.94	43.74	○	○	○
BALD1	Mount Baldy	US	I	-109.44	34.06	○	○	○
BAND1	Bandelier NM	US	I	-106.27	35.78	○	○	○
BIBE1	Big Bend NP	US	I	-103.18	29.30	○	○	○
BIRM1	North Birmingham	US	I	-86.81	33.55	○	○	○
BLIS1	Bliss SP (TRPA)	US	I	-120.10	38.98	○	○	○
BLMO1	Blue Mounds	US	I	-96.19	43.72	○	○	○
BOAP1	Bosque del Apache	US	I	-106.85	33.87	○	○	○
BOLA1	Boulder Lake	US	I	-109.64	42.85	○	○	○
BOND1	Bondville	US	I	-88.37	40.05	○	○	○
BOWA1	Boundary Waters Canoe Area	US	I	-91.50	47.95	○	○	○
BRCA1	Bryce Canyon NP	US	I	-112.17	37.62	○	○	○
BRID1	Bridger Wilderness	US	I	-109.76	42.97	○	○	○
BRIG1	Brigantine NWR	US	I	-74.45	39.47	○	○	○
BRIS1	Breton Island	US	I	-89.76	30.11	○	○	○
BRMA1	Bridgton	US	I	-70.73	44.11	○	○	○
CABA1	Casco Bay	US	I	-70.06	43.83	○	○	○
CABI1	Cabinet Mountains	US	I	-115.67	47.95	○	○	○
CACO1	Cape Cod	US	I	-70.02	41.98	○	○	○
CACR1	Caney Creek	US	I	-94.14	34.45	○	○	○
CADI1	Cadiz	US	I	-87.85	36.78	○	○	○
CANY1	Canyonlands NP	US	I	-109.82	38.46	○	○	○
CAPI1	Capitol Reef NP	US	I	-111.29	38.30	○	○	○
CEBL1	Cedar Bluff	US	I	-99.76	38.77	○	○	○
CHAS1	Chassahowitzka NWR	US	I	-82.55	28.75	○	○	○
CHER1	Cherokee Nation	US	I	-97.03	36.96	○	○	○
CHIR1	Chiricahua NM	US	I	-109.39	32.01	○	○	○
CLPE1	Cloud Peak	US	I	-106.96	44.33	○	○	○
COGO1	Columbia Gorge #1	US	I	-122.21	45.57	○	○	○
COHU1	Cohutta	US	I	-84.63	34.79	○	○	○
CORI1	Columbia River Gorge	US	I	-121.00	45.66	○	○	○
CRES1	Crescent Lake	US	I	-102.43	41.76	○	○	○
CRMO1	Craters of the Moon NM	US	I	-113.56	43.46	○	○	○
DENA1	Denali NP	US	I	-148.97	63.72	○	○	○
DETR1	Detroit	US	I	-83.21	42.23	○	○	○
DEVA1	Death Valley NP	US	I	-116.85	36.51	○	○	○
DOME1	Dome Lands Wilderness	US	I	-118.14	35.73	○	○	○
DOSO1	Dolly Sods Wilderness	US	I	-79.43	39.11	○	○	○
DOUG1	Douglas	US	I	-109.54	31.35	○	○	○
EGBE1	Egbert	US	I	-79.78	44.23	○	○	○
ELDO1	El Dorado Springs	US	I	-94.03	37.70	○	○	○
ELLI1	Ellis	US	I	-99.94	36.09	○	○	○
EVER1	Everglades NP	US	I	-80.68	25.39	○	○	○
FLAT1	Flathead	US	I	-114.27	47.77	○	○	○
FOPE1	Fort Peck	US	I	-105.10	48.31	○	○	○

FRES1	Fresno	US	I	-119.77	36.78	○	○	○
FRRE1	Frostberg Reservoir (Big Piney Run)	US	I	-79.01	39.71	○	○	○
GAAR1	Gates of the Arctic NP	US	I	-151.52	66.90	○	○	○
GAMO1	Gates of the Mountains	US	I	-111.71	46.83	○	○	○
GICL1	Gila Wilderness	US	I	-108.24	33.22	○	○	○
GLAC1	Glacier NP	US	I	-114.00	48.51	○	○	○
GRBA1	Great Basin NP	US	I	-114.22	39.01	○	○	○
GRCA2	Hance Camp at Grand Canyon NP	US	I	-111.98	35.97	○	○	○
GRGU1	Great Gulf Wilderness	US	I	-71.22	44.31	○	○	○
GRRI1	Great River Bluffs	US	I	-91.41	43.94	○	○	○
GRSA1	Great Sand Dunes NM	US	I	-105.52	37.72	○	○	○
GRSM1	Great Smoky Mountains NP	US	I	-83.94	35.63	○	○	○
GUMO1	Guadalupe Mountains NP	US	I	-104.81	31.83	○	○	○
HACR1	Haleakala Crater	US	I	-156.25	20.76	○	○	○
HALE1	Haleakala NP	US	I	-156.28	20.81	○	○	○
HAVO1	Hawaii Volcanoes NP	US	I	-155.26	19.43	○	○	○
HECA1	Hells Canyon	US	I	-116.84	44.97	○	○	○
HEGL1	Hercules-Glades	US	I	-92.92	36.61	○	○	○
HOOV1	Hoover	US	I	-119.18	38.09	○	○	○
IKBA1	Ike's Backbone	US	I	-111.68	34.34	○	○	○
INGA1	Indian Gardens	US	I	-112.13	36.08	○	○	○
ISLE1	Isle Royale NP	US	I	-88.15	47.46	○	○	○
JARB1	Jarbidge Wilderness	US	I	-115.43	41.89	○	○	○
JARI1	James River Face Wilderness	US	I	-79.51	37.63	○	○	○
JOSH1	Joshua Tree NP	US	I	-116.39	34.07	○	○	○
KAIS1	Kaiser	US	I	-119.15	37.22	○	○	○
KALM1	Kalmiopsis	US	I	-124.06	42.55	○	○	○
LABE1	Lava Beds NM	US	I	-121.51	41.71	○	○	○
LASU2	Lake Sugema	US	I	-92.01	40.69	○	○	○
LAVO1	Lassen Volcanic NP	US	I	-121.58	40.54	○	○	○
LIGO1	Linville Gorge	US	I	-81.93	35.97	○	○	○
LIVO1	Livonia	US	I	-86.26	38.53	○	○	○
LOST1	Lostwood	US	I	-102.40	48.64	○	○	○
LYBR1	Lye Brook Wilderness	US	I	-73.13	43.15	○	○	○
MACA1	Mammoth Cave NP	US	I	-86.15	37.13	○	○	○
MAKA1	Makah Tribe	US	I	-124.60	48.37	○	○	○
MAVI1	Martha's Vineyard	US	I	-70.78	41.33	○	○	○
MEAD1	Meadview	US	I	-114.07	36.02	○	○	○
MELA1	Medicine Lake	US	I	-104.48	48.49	○	○	○
MEVE1	Mesa Verde NP	US	I	-108.49	37.20	○	○	○
MING1	Mingo	US	I	-90.14	36.97	○	○	○
MKGO1	M.K. Goddard	US	I	-80.15	41.43	○	○	○
MOHO1	Mount Hood	US	I	-121.78	45.29	○	○	○
MOMO1	Mohawk Mt.	US	I	-73.30	41.82	○	○	○
MONT1	Monture	US	I	-113.15	47.12	○	○	○
MOOS1	Moosehorn NWR	US	I	-67.27	45.13	○	○	○
MORA1	Mount Rainier NP	US	I	-122.12	46.76	○	○	○
MOZI1	Mount Zirkel Wilderness	US	I	-106.68	40.54	○	○	○
NEBR1	Nebraska NF	US	I	-100.34	41.89	○	○	○
NEYO1	Is 52	US	I	-73.90	40.82	○	○	○
NOAB1	North Absaroka	US	I	-109.38	44.74	○	○	○
NOCA1	North Cascades	US	I	-121.06	48.73	○	○	○
NOCH1	Northern Cheyenne	US	I	-106.56	45.65	○	○	○

OKEF1	Okefenokee NWR	US	I	-82.13	30.74	◯	◯	◯
OLYM1	Olympic	US	I	-122.97	48.01	◯	◯	◯
ORPI1	Organ Pipe	US	I	-112.80	31.95	◯	◯	◯
PACK1	Pack Monadnock Summit	US	I	-71.88	42.86	◯	◯	◯
PASA1	Pasayten	US	I	-119.93	48.39	◯	◯	◯
PEFO1	Petrified Forest NP	US	I	-109.77	35.08	◯	◯	◯
PENO1	Penobscot	US	I	-68.65	44.95	◯	◯	◯
PHOE1	Phoenix	US	I	-112.10	33.50	◯	◯	◯
PINN1	Pinnacles NM	US	I	-121.16	36.48	◯	◯	◯
PITT1	Lawrenceville	US	I	-79.96	40.47	◯	◯	◯
PMRF1	Proctor Maple R. F.	US	I	-72.87	44.53	◯	◯	◯
PORE1	Point Reyes National Seashore	US	I	-122.91	38.12	◯	◯	◯
PRIS1	Presque Isle	US	I	-68.03	46.70	◯	◯	◯
PUSO1	Puget Sound	US	I	-122.31	47.57	◯	◯	◯
QUCI1	Quaker City	US	I	-81.34	39.94	◯	◯	◯
QURE1	Quabbin Summit	US	I	-72.33	42.30	◯	◯	◯
QUVA1	Queen Valley	US	I	-111.29	33.29	◯	◯	◯
RAFA1	San Rafael	US	I	-120.01	34.73	◯	◯	◯
REDW1	Redwood NP	US	I	-124.08	41.56	◯	◯	◯
ROMA1	Cape Romain NWR	US	I	-79.66	32.94	◯	◯	◯
ROMO1	Rocky Mountain NP	US	I	-105.55	40.28	◯	◯	◯
SACR1	Salt Creek	US	I	-104.40	33.46	◯	◯	◯
SAFO1	Sac and Fox	US	I	-95.57	39.98	◯	◯	◯
SAGO1	San Gorgonio Wilderness	US	I	-116.91	34.19	◯	◯	◯
SAGU1	Saguaro NM	US	I	-110.74	32.17	◯	◯	◯
SAMA1	St. Marks	US	I	-84.16	30.09	◯	◯	◯
SAPE1	San Pedro Parks	US	I	-106.84	36.01	◯	◯	◯
SAWE1	Saguaro West	US	I	-111.22	32.25	◯	◯	◯
SAWT1	Sawtooth NF	US	I	-114.93	44.17	◯	◯	◯
SENE1	Seney	US	I	-85.95	46.29	◯	◯	◯
SEQU1	Sequoia NP	US	I	-118.83	36.49	◯	◯	◯
SHEN1	Shenandoah NP	US	I	-78.43	38.52	◯	◯	◯
SHMI1	Shamrock Mine	US	I	-107.48	37.30	◯	◯	◯
SHRO1	Shining Rock Wilderness	US	I	-82.77	35.39	◯	◯	◯
SIAN1	Sierra Ancha	US	I	-110.94	34.09	◯	◯	◯
SIKE1	Sikes	US	I	-92.44	32.06	◯	◯	◯
SIME1	Simeonof	US	I	-160.51	55.33	◯	◯	◯
SIPS1	Sipsey Wilderness	US	I	-87.34	34.34	◯	◯	◯
SNPA1	Snoqualmie Pass	US	I	-121.43	47.42	◯	◯	◯
STAR1	Starkey	US	I	-118.51	45.22	◯	◯	◯
SULA1	Sula Peak	US	I	-114.00	45.86	◯	◯	◯
SWAN1	Swanquarter	US	I	-76.21	35.45	◯	◯	◯
SYCA1	Sycamore Canyon	US	I	-111.97	35.14	◯	◯	◯
TALL1	Tallgrass	US	I	-96.56	38.43	◯	◯	◯
THBA1	Thunder Basin	US	I	-105.29	44.66	◯	◯	◯
THRO1	Theodore Roosevelt	US	I	-103.38	46.89	◯	◯	◯
THSI1	Three Sisters Wilderness	US	I	-122.04	44.29	◯	◯	◯
TONT1	Tonto NM	US	I	-111.11	33.65	◯	◯	◯
TRCR1	Trapper Creek	US	I	-150.32	62.32	◯	◯	◯
TRIN1	Trinity	US	I	-122.80	40.79	◯	◯	◯
TUXE1	Tuxedni	US	I	-152.67	59.99	◯	◯	◯
ULBE1	UL Bend	US	I	-108.72	47.58	◯	◯	◯
UPBU1	Upper Buffalo Wilderness	US	I	-93.20	35.83	◯	◯	◯

VIIS1	Virgin Islands NP	US	I	-64.80	18.34	○	○	○
VILA1	Viking Lake	US	I	-95.05	40.97	○	○	○
VOYA2	Voyageurs NP #2	US	I	-92.83	48.41	○	○	○
WASH1	Washington D.C.	US	I	-77.03	38.88	○	○	○
WEMI1	Weminuche Wilderness	US	I	-107.80	37.66	○	○	○
WHIT1	White Mountain	US	I	-105.53	33.47	○	○	○
WHPA1	White Pass	US	I	-121.39	46.62	○	○	○
WHPE1	Wheeler Peak	US	I	-105.45	36.59	○	○	○
WHRI1	White River NF	US	I	-106.82	39.15	○	○	○
WICA1	Wind Cave	US	I	-103.48	43.56	○	○	○
WIMO1	Wichita Mountains	US	I	-98.71	34.73	○	○	○
WRIG1	Wrightwood	US	I	-117.69	34.38	○	○	○
YELL2	Yellowstone NP 2	US	I	-110.40	44.57	○	○	○
YOSE1	Yosemite NP	US	I	-119.71	37.71	○	○	○
ZICA1	Zion Canyon	US	I	-113.15	37.20	○	○	○
CH0002R	Payerne	Switzerland	EM	6.94	46.81	○	○	○
CH0005R	Rigi	Switzerland	EM	8.46	47.07	○	○	○
DE0002R	Waldhof	Germany	EM	10.76	52.80	○	○	○
DE0003R	Schauinsland	Germany	EM	7.91	47.91	○	○	○
DE0007R	Neuglobsow	Germany	EM	13.03	53.17	○	○	○
DE0008R	Schmücke	Germany	EM	10.77	50.65	○	○	○
DE0044R	Melpitz	Germany	EM	12.93	51.53	○	○	○
ES0009R	Campisabalos	Spain	EM	-3.14	41.28	○	○	○
ES1778R	Montseny	Spain	EM	2.35	41.77	○	○	○
FR0030R	Puy de Dome	France	EM	2.95	45.77	○	○	○
GB0036R	Harwell	UK	EM	-1.32	51.57	○	○	○
IT0004R	Ispra	Italy	EM	8.63	45.80	○	○	○
NL0114U	Overtoom	Netherlands	EM	4.81	52.36	○	○	○
NL0118K	Ring_A10_Zuid	Netherlands	EM	4.90	52.33	○	○	○
NO0001R	Birkenes	Norway	EM	8.25	58.38	○	○	○
NO0002R	Birkenes II	Norway	EM	8.25	58.39	○	○	○
NO0039R	Kårvatn	Norway	EM	8.88	62.78	○	○	○
NO0056R	Hurdal	Norway	EM	11.08	60.37	○	○	○
PL0005R	Diabla Gora	Poland	EM	22.07	54.15	○	○	○
SE0011R	Vavihill	Sweden	EM	13.15	56.02	○	○	○
SE0012R	Aspvreten	Sweden	EM	17.38	58.80	○	○	○
SI0008R	Iskrba	Slovenia	EM	14.87	45.57	○	○	○
CD	Chengdu	China	C	104.04	30.65	○	○	○
DL	Dalian	China	C	121.63	38.90	○	○	○
DH	Dunhuang	China	C	94.68	40.15	○	○	○
GLS	Gaolanshan	China	C	105.85	36.00	○	○	○
GC	Gucheng	China	C	115.80	39.13	○	○	○
JS	Jinsha	China	C	114.20	29.63	○	○	○
LS	Lhasa	China	C	91.13	29.67	○	○	○
LA	LinAn	China	C	119.73	30.30	○	○	○
LFS	Longfengshan	China	C	127.60	44.73	○	○	○
NJ	Nanning	China	C	108.35	22.82	○	○	○
PY	Panyu	China	C	113.35	23.00	○	○	○
TYS	Taiyangshan	China	C	111.71	29.17	○	○	○
XA	Xian	China	C	108.97	34.43	○	○	○
ZZ	Zhengzhou	China	C	113.68	34.78	○	○	○
CRLA1	Crater Lake NP	US	I	-122.14	42.90	○	○	
CY0002R	Ayia Marina	Cyprus	E	33.06	35.04	○	○	

CZ0003R	Kosetice	Czech	E	15.08	49.57	○	○	
BIBE1	Big Bend NP	US	I	-103.18	29.30			○
BIRM1	North Birmingham	US	I	-86.81	33.55			○
BRET1	Breton	US	I	-89.21	29.12			○
CHIC1	Chicago	US	I	-87.71	41.75			○
COHI1	Connecticut Hill	US	I	-76.65	42.40			○
FLTO1	Flat Tops	US	I	-107.63	39.92			○
HILL1	Hillside	US	I	-112.96	34.43			○
HOUS1	Houston Deer Park #2	US	I	-95.13	29.67			○
LTCC1	Lake Tahoe Community College	US	I	-119.97	38.92			○
OLTO1	Old Town	US	I	-68.65	44.93			○
OMAH1	Omaha	US	I	-96.43	42.15			○
OWVL1	Owens Valley	US	I	-118.33	37.36			○
PETE1	Petersburg	US	I	-132.81	56.61			○
PHOE5	Phoenix Colocated Sampler	US	I	-112.10	33.50			○
ROMA1	Cape Romain NWR	US	I	-79.66	32.94			○
RUBI1	Rubidoux	US	I	-117.42	34.00			○
SAGA1	San Gabriel	US	I	-118.03	34.30			○
SPOK1	Spokane Res.	US	I	-117.86	47.90			○
STIL1	Stilwell	US	I	-94.67	35.75			○
WARI1	Walker River Paiute Tribe	US	I	-118.81	38.95			○
AM0001R	Amberd	Armenia	EM	44.26	40.38			○
AT0002	Illmitz	Austria	EM	16.77	47.77			○
DE0001	Westerland	Germany	EM	8.31	54.93			○
DE0009	Zingst	Germany	EM	12.73	54.43			○
DK0003	Tange	Denmark	EM	9.60	56.35			○
DK0005	Keldsnor	Denmark	EM	10.73	54.73			○
DK0008	Anholt	Denmark	EM	11.52	56.72			○
DK0010	Nord, Greenland	Denmark	EM	-16.67	81.60			○
DK0012	Risoe	Denmark	EM	12.09	55.69			○
DK0031	Ulborg	Denmark	EM	8.43	56.28			○
FI0009	Utö	Finland	EM	21.38	59.78			○
FI0017	Virolahti II	Finland	EM	27.69	60.53			○
FI0022	Oulanka	Finland	EM	29.40	66.32			○
FI0036	Pallas (Matorova)	Finland	EM	24.24	68.00			○
FI0037	Ähtäri II	Finland	EM	24.18	62.58			○
IE0001	Valentia Observatory	Ireland	EM	-10.24	51.94			○
IE0005	Oak Park	Ireland	EM	-6.92	52.87			○
IE0006	Malin Head	Ireland	EM	-7.34	55.38			○
IE0008	Carnsore Point	Ireland	EM	-6.37	52.19			○
IS0002	Irafoss	Iceland	EM	-21.02	64.08			○
IS0091	Storhofdi	Iceland	EM	-20.28	63.40			○
LV0010	Rucava	Latvia	EM	21.17	56.16			○
MD0013	Leova II	Moldova	EM	28.28	46.49			○
NL0008	Bilthoven	Netherlands	EM	5.20	52.12			○
NL0009	Kollumerwaard	Netherlands	EM	6.28	53.33			○
NL0010	Vredepeel	Netherlands	EM	5.85	51.54			○
NL0091	De Zilk	Netherlands	EM	4.50	52.30			○
NO0015	Tustervatn	Norway	EM	13.92	65.83			○
NO0042	Ny-Ålesund	Norway	EM	11.89	78.91			○
NO0055	Karasjok	Norway	EM	25.22	69.47			○
NO0090	Andøya	Norway	EM	16.01	69.28			○
NO0091	Søgne	Norway	EM	7.85	58.12			○

SE0014	Råö	Sweden	EM	11.91	57.39	○
SK0002	Chopok	Slovakia	EM	19.58	48.93	○
SK0004	Stará Lesná	Slovakia	EM	20.28	49.15	○
SK0006	Starina	Slovakia	EM	22.27	49.05	○
-	Phnom Penh	Cambodia	EA	104.83	11.55	○
-	Hongwen	China	EA	118.13	24.47	○
-	Serpong	Indonesia	EA	106.57	-6.25	○
-	Rishiri	Japan	EA	141.21	45.12	○
-	Ochiishi	Japan	EA	145.50	43.15	○
-	Tappi	Japan	EA	140.35	41.25	○
-	Sadoseki	Japan	EA	138.40	38.23	○
-	Happo	Japan	EA	137.80	36.68	○
-	Ijira	Japan	EA	136.69	35.57	○
-	Oki	Japan	EA	133.19	36.28	○
-	Banryu	Japan	EA	131.80	34.67	○
-	Yusuhara	Japan	EA	132.93	33.37	○
-	Hedo	Japan	EA	128.25	26.85	○
-	Ogasawara	Japan	EA	142.22	27.08	○
-	Tokyo	Japan	EA	139.76	35.68	○
-	TanahRata	Malaysia	EA	101.38	4.47	○
-	Petaling Jaya	Malaysia	EA	101.65	3.10	○
-	Danum Valley	Malaysia	EA	117.85	4.98	○
-	Ulaanbaatar	Mongolia	EA	106.82	47.90	○
-	Terelj	Mongolia	EA	107.48	47.98	○
-	Yangon	Myanmar	EA	96.12	16.50	○
-	Metro Manila	Philippines	EA	121.07	14.63	○
-	Los Banos	Philippines	EA	121.25	14.18	○
-	Mt. Sto. Tomas	Philippines	EA	120.60	16.42	○
-	Mondy	Russia	EA	101.00	51.67	○
-	Listvyanka	Russia	EA	104.90	51.85	○
-	Irkutsk	Russia	EA	104.25	52.23	○
-	Primorskaya	Russia	EA	132.12	43.70	○
-	Bangkok	Thailand	EA	100.53	13.77	○
-	Patumthani	Thailand	EA	100.57	13.73	○
-	Khanchanaburi	Thailand	EA	100.77	14.03	○
-	Chiang Mai	Thailand	EA	98.93	18.77	○
-	Nakhon Ratchasima	Thailand	EA	101.88	14.45	○
-	Ha Noi	Viet Nam	EA	105.85	21.02	○
-	Hoa Binh	Viet Nam	EA	105.33	20.82	○
BYIS1	Baengnyeong Island	Korea	I	124.63	37.97	○

#1 Network includes I (IMPROVE), EM (EMEP), C (CAWNET) and EA (EANET).

Table S3: Observation sites of dust and sea salt operated by University of Miami, US.

Site	Country	LON	LAT	dust	sea salt
Midway Island	US	-177.40	28.20	○	○
Oahu Hawaii	US	-157.70	21.30	○	○
RSMAS Univ. of Miami	US	-80.20	25.80	○	○
Ragged Point	Barbados	-59.40	13.20	○	○
Mace Head	Ireland	-9.90	53.30	○	○
Cape Point	S. Africa	18.50	-34.30	○	○
Cheju	Korea	126.50	33.50	○	○
Hedo Okinawa	Japan	128.20	26.90	○	○
Cape Grim Tasmania	Australia	144.70	-40.70	○	○
Norfolk Island	Australia	168.00	-29.10	○	○
Funafuti	Tuvalu	-179.00	-8.50	○	
Bermuda	UK	-64.90	32.30	○	
Marsh-King George island	Antarctica	-58.30	-62.20	○	
Izana Tenerife	Spain	-16.50	28.30	○	
Mawson	Antarctica	62.50	-67.60	○	
Enewetak Atoll	US	162.30	11.30	○	
Yate	New Caledonia	167.00	-22.10	○	
Nauru	Nauru	167.00	-0.50	○	
Chatham Island	New Zealand	-176.50	-43.90		○
America Samoa	US	-170.60	-14.20		○
Fanning Island	Kiribati	-159.30	3.90		○
Palmer	Antarctica	-64.05	-64.90		○
Heimaey	Iceland	-20.30	63.40		○
Reunion Island	France	55.83	-21.20		○
Invercargill	New Zealand	168.40	-46.40		○
Wellington	New Zealand	174.90	-41.30		○

Table S4: Observation sites of surface radiation fluxes by BSRN.

Code	Site	Country	LON	LAT
ale	Alert	US	-62.42	82.49
ber	Bermuda	US	-64.67	32.27
bon	Bondville	US	-88.37	40.07
bos	Boulder, SURFRAD	US	-105.24	40.13
bou	Boulder	US	-105.01	40.05
clh	Chesapeake Light	US	-75.71	36.91
dra	Desert Rock	US	-116.02	36.63
fpe	Fort Peck	US	-105.10	48.32
cab	Cabauw	Netherlands	4.93	51.97
car	Carpentras	France	5.06	44.08
nya	Ny-Ålesund	Norway	11.93	78.93
pal	Palaiseau	France	2.21	48.71
tor	Toravere	Estonia	26.46	58.25
sbo	Sedo Boqer	Israel	34.78	30.86
tam	Tamanrasset	Algeria	5.53	22.79
asp	Alice Springs	Australia	133.89	-23.80
dar	Darwin	Australia	130.89	-12.43
dom	Concordia Station	Antarctica	123.38	-75.10
dwn	Darwin Met Office	Australia	130.89	-12.42
gvn	Neumayer Station	Antarctica	-8.25	-70.65
lau	Lauder	New Zealand	169.69	-45.05
man	Momote	Papua New Guinea	147.43	-2.06
nau	Nauru Island	Nauru	166.92	-0.52
syo	Syowa	Antarctica	39.59	-69.01
tat	Tateno	Japan	140.13	36.06

Table S5: Statistical metrics (Sampling number: N, Pearson correlation coefficient: PCC, root-mean-square error: RMSE and normalized mean bias: NMB) for the AOT at a wavelength of 500 nm between satellite measurements (AERONET, SKYNET, CARSNET) and the NICAM (the HRM with the original grid of 0.125°×0.125°, the HRM with the interpolated grid of 0.5°×0.5°, i.e., denoted as 'HRM with 0.5° average', the LRM with the original grid of 0.5°×0.5°) simulations for the annual, January and July averages. The HRM and LRM results are plotted in Figure 6. The comparison sites are shown in Figure 1(b) and Table S1.

	HRM (0.125°)	**HRM with 0.5° average**	**LRM (0.5°)**
		Annual	
N	91	91	91
PCC	0.471	0.457	0.356
RMSE	0.209	0.212	0.237
NMB (%)	-20.2	-21.0	-26.6
		January	
N	83	83	83
PCC	0.589	0.579	0.569
RMSE	0.233	0.236	0.238
NMB (%)	-44.1	-44.9	-45.7
		July	
N	136	136	136
PCC	0.475	0.468	0.403
RMSE	0.233	0.233	0.299
NMB (%)	-5.4	-6.1	-11.6

Table S6: Statistical metrics (N, PCC, RMSE and NMB) for the surface aerosol mass concentrations (sulfate, BC and POM) between satellite measurements (IMPROVE, EMEP, EANET and CAWNET) and the NICAM (the HRM with the original grid of 0.125°×0.125°, the HRM with the interpolated grid of 0.5°×0.5°, i.e., denoted as 'HRM with 0.5° average', the LRM with the original grid of 0.5°×0.5°) simulations for the annual averages. The HRM and LRM results are plotted in Figure 8. The site information is shown in Figure 1(a) and Table S2.

	HRM (0.125°)	**HRM with 0.5° average**	**LRM (0.5°)**
		Sulfate	
N	285	285	285
PCC	0.812	0.785	0.764
RMSE	4.04	4.19	4.44
NMB (%)	-15.1	-15.6	-24.1
		BC	
N	210	210	210
PCC	0.890	0.879	0.869
RMSE	1.16	1.25	1.28
NMB (%)	-46.4	-51.1	-52.7
		POM	
N	210	210	210
PCC	0.819	0.800	0.794
RMSE	5.03	5.18	5.21
NMB (%)	-54.8	-56.2	-56.1

Table S7: Statistical metrics (N, PCC, RMSE and NMB) for the surface aerosol mass concentrations (dust) between the measurements (the network managed by the University of Miami) and the NICAM (the HRM with the original grid of 0.125°×0.125°, the HRM with the interpolated grid of 0.5°×0.5°, i.e., denoted as 'HRM with 0.5° average', the LRM with the original grid of 0.5°×0.5°) simulations for the annual, January and July averages. The HRM and LRM results are plotted in Figure 9. The site information is shown in Figure 1(a) and Table S3.

	HRM (0.125°)	**HRM with 0.5° average**	**LRM (0.5°)**
		Annual	
N	18	18	18
PCC	0.895	0.895	0.898
RMSE	4.08	4.03	3.85
NMB (%)	-28.8	-29.2	-35.3
		January	
N	17	17	17
PCC	0.639	0.640	0.660
RMSE	9.03	8.89	4.26
NMB (%)	37.4	35.9	-22.3
		July	
N	18	18	18
PCC	0.752	0.721	0.682
RMSE	10.61	10.69	10.24
NMB (%)	-64.8	-63.8	-55.6

Table S8: Same as Table S7, but for sea salt

	HRM (0.125°)	**HRM with 0.5° average**	**LRM (0.5°)**
		Annual	
N	18	18	18
PCC	0.258	0.263	0.263
RMSE	7.84	7.84	8.92
NMB (%)	-26.1	-25.3	-37.7
		January	
N	18	18	18
PCC	0.616	0.599	0.368
RMSE	8.22	8.26	10.59
NMB (%)	-29.0	-27.7	-40.9
		July	
N	18	18	18
PCC	0.153	0.128	0.233
RMSE	7.70	7.86	7.93
NMB (%)	-17.9	-15.9	-30.7

Table S9: Calculation cost for HRM and LRM in seconds per daily integration. The value in parentheses represents the contribution to the total cost.

Process		HRM	LRM
Dynamics	**Tracer advection**	56 (20%)	402 (12%)
	Other	61 (22%)	325 (12%)
Physics	**Microphysics**	56 (20%)	1035 (39%)
	Radiation	25 (9%)	243 (9%)
	Aerosol	27 (10%)	296 (11%)
	Surface flux + Turbulence	16 (6%)	182 (7%)
	Other	14 (5%)	134 (5%)
Other		22 (8%)	58 (2%)
Total		278 (100%)	2675 (100%)

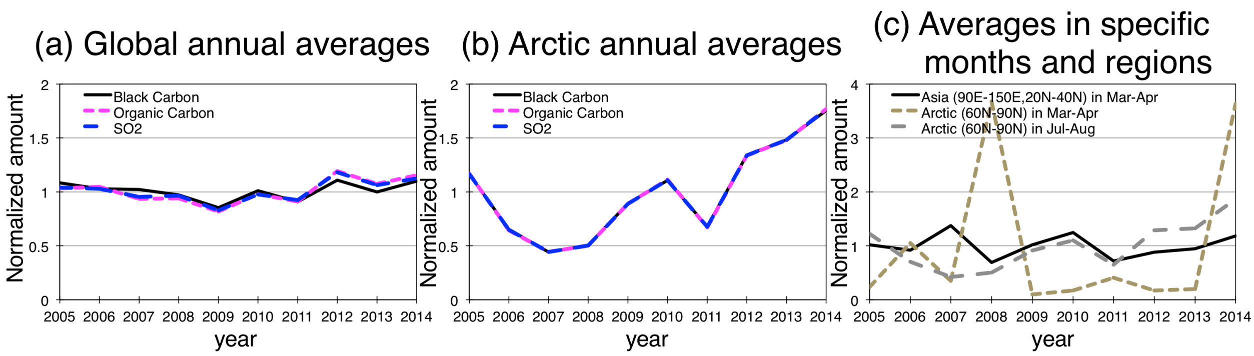

Figure S1: Interannual variabilities of emission fluxes for BC, OC and SO_2 from biomass burning over 2005-2014 from the Global Fire Emission Database version 4 (GFEDv4; van der Werf et al., 2017) using normalized amounts of the emission by that in the 2005-2014 average in (a) global annual averages, (b) annual averages in Arctic (60°N-90°N) and (c) BC averages in specific months and regions including Asia (90°E-150°E, 20°N-40°N) in March-April, Arctic (60°N-90°N) in March-April and Arctic (60°N-90°N) in July-August. The target months and regions are compared in the vertical BC distribution by using flight observations in Figure 14.

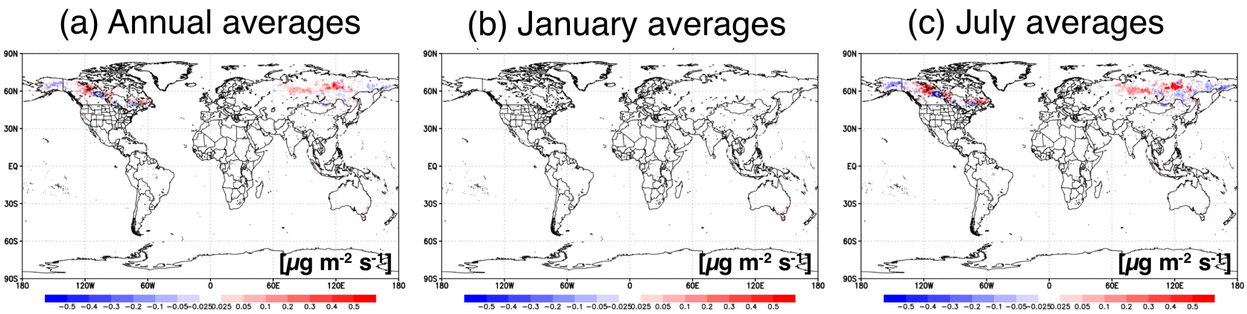

Figure S2: Differences in BC emission fluxes from biomass burning by GFEDv4 between the 2012-2014 and the 2005-2014 averages, i.e., 2012-2014 averages minus 2005-2014 averages, in the (a) annual, (b) January and (c) July averages. All units are in μg m^{-2} s^{-1}.

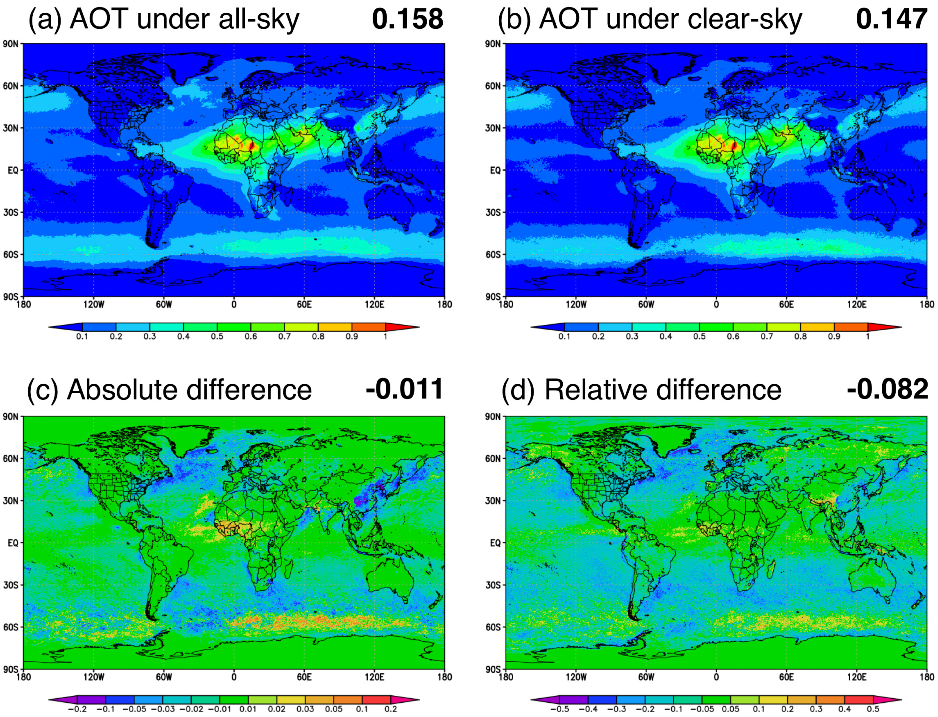

Figure S3: Global distributions of the 1-year averages of (a) the HRM-simulated AOT under the all-sky conditions, (b) the HRM-simulated AOT under the clear-sky conditions, (c) the absolute difference between the HRM-simulated AOT under the all-sky and clear-sky conditions, i.e., AOT(clear-sky) minus AOT (all-sky), and (d) the relative difference between the HRM-simulated AOT under the all-sky and clear-sky conditions, i.e., the ratio of the absolute difference to AOT (all-sky), with the original grid (0.125°×0.125°). The numbers shown in the upper-right corner in each panel represent the global averages.

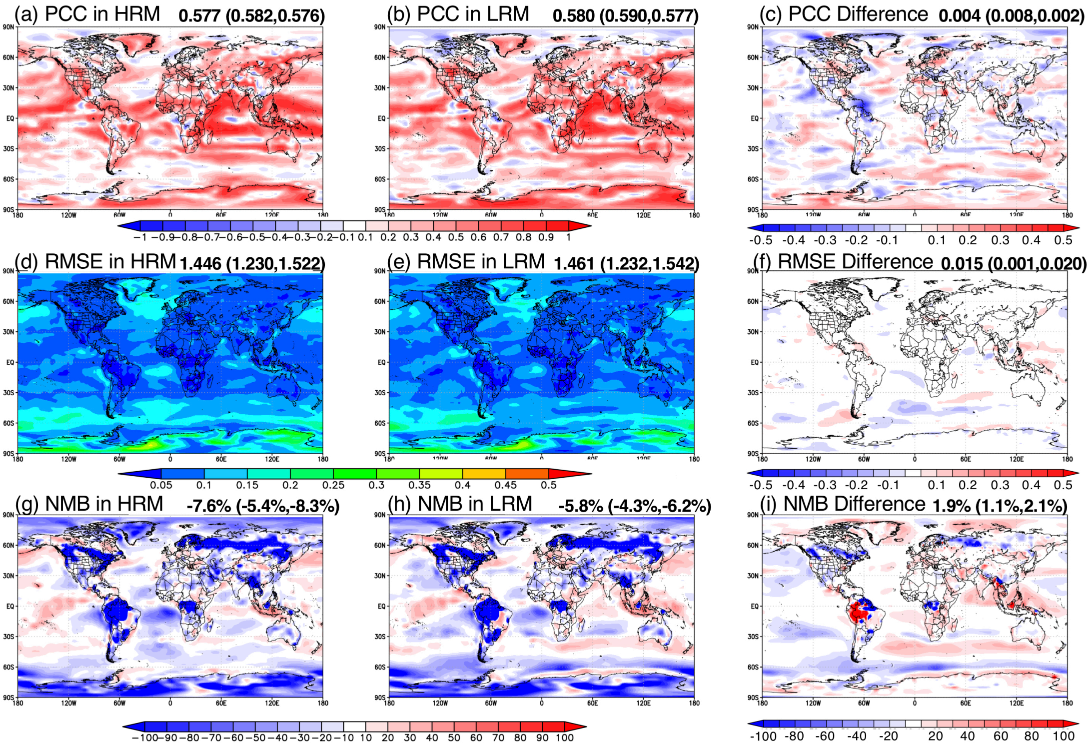

Figure S4: Global distributions of the statistical metrics, i.e., the (a,b) Pearson correlation coefficient (PCC), (d,e) root-mean-square error (RMSE) and (g,h) normalized mean bias (NMB), for wind speed at 10-m height between the NICAM (HRM and LRM) simulations and NCEP reanalysis for the annual averages and (c,f,i) the differences in these metrics between the HRM and LRM, i.e., LRM minus HRM. These metrics are calculated using data representing 12-monthly averages over three years in each grid (2.5°×2.5°). The numbers shown in the upper-right corner without the brackets in each panel represent global averages using the 12-monthly averages; those in brackets represent the global land and ocean averages.

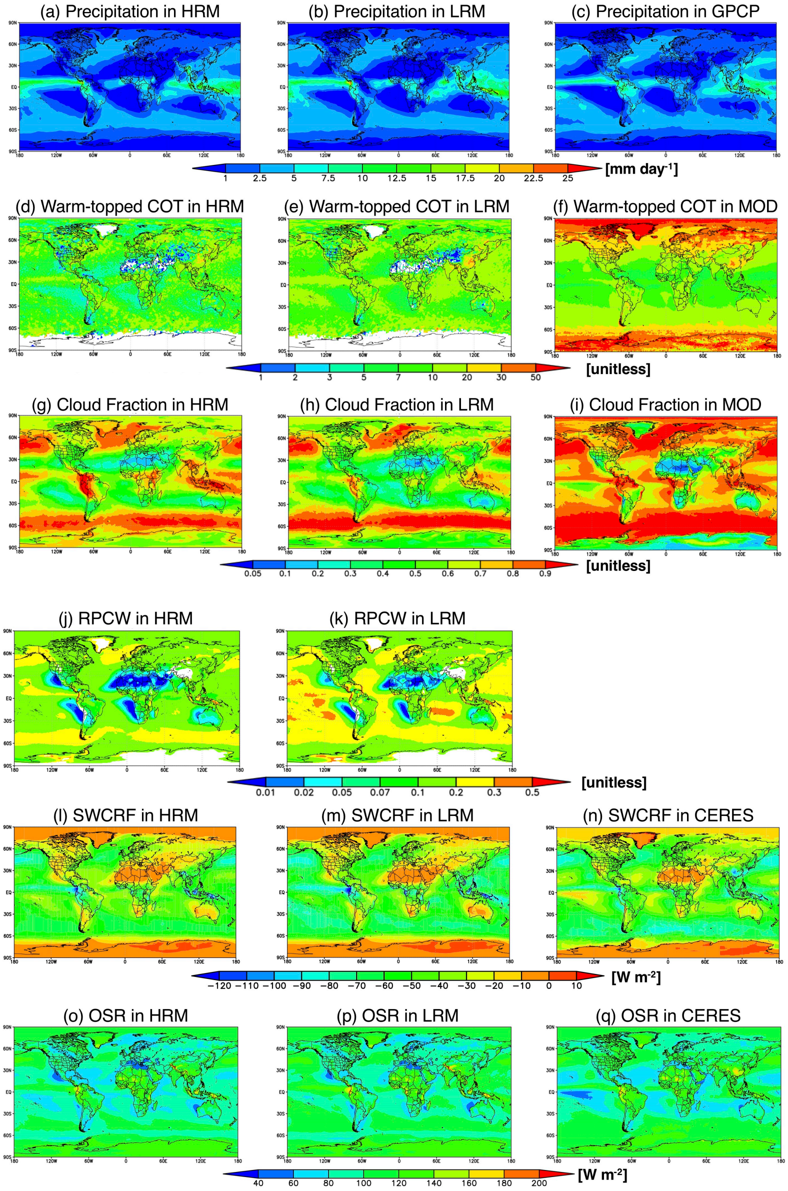

Figure S5: Global distributions of the annual averages of (a,b,c) precipitation, (d,e,f) cloud optical thickness (COT) for warm-topped clouds, (g,h,i) cloud fraction (CF) in all types of clouds, (j,k) ratio of precipitation to total cloud water (RPCW) at a height of 2 km, (l,m,n) shortwave cloud radiative forcing (SWCRF) and (o,p,q) outgoing shortwave radiation flux (OSR) simulated by the HRM and LRM, reanalyzed by the GPCP only in precipitation with a grid of 2.5°×2.5°, retrieved from both MODIS/Terra (MOD) in warm-topped COT and CF with a grid of 1°×1°, and estimated by CERES in SWCRF and OSR with a grid of 1°×1°. The annual averages of these variables except for CF and COT are calculated by a 3-year integration, whereas those in CF and COT are calculated by a 1-year integration using 6-hourly instantaneous clouds at 12:00 (local time) to more exactly compare them with the MODIS/Terra observation at approximately 10:30 (local time). The units are described in each panel.

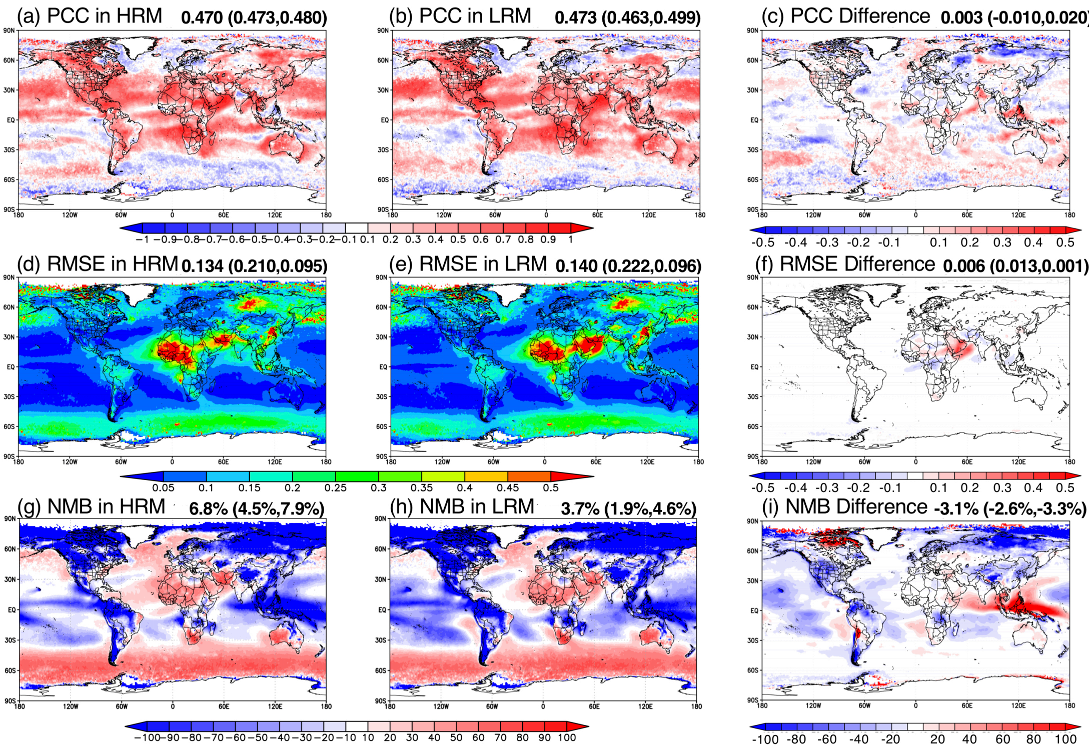

Figure S6: Same as Figure S5, but for AOT using a reference of MODIS/Aqua retrievals with a grid of 1°×1°. The global averages are calculated using grids (60°S-60°N) without undefined grids in MODIS/Aqua.

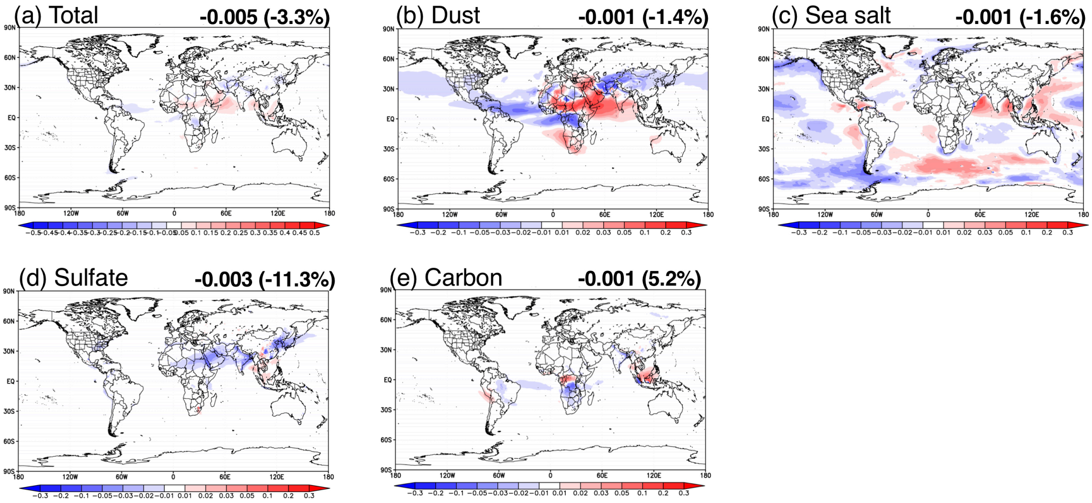

Figure S7: Global distributions of the differences in the (a) total AOT and (b,c,d,e) AOT components (dust, sea salt, sulfate and total carbonaceous aerosols, respectively) between the HRM and LRM (LRM minus HRM) for the annual averages with a grid of 0.5°×0.5°. The numbers shown in upper-right corner in each panel represent the annual and global averages of the difference, and the numbers in brackets represent the annual and global averages of the relative difference in units of %.

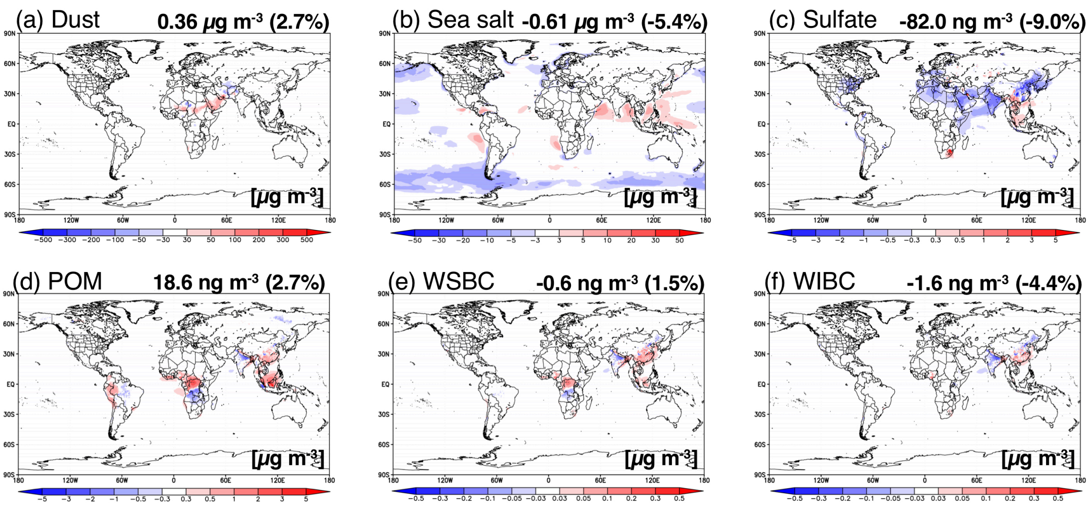

Figure S8: Global distribution of the differences in the surface mass concentrations of (a) dust, (b) sea salt, (c) sulfate, (d) POM, (e) WSBC and (f) WIBC between the HRM and LRM (LRM minus HRM) for the annual averages with a grid of 0.5°×0.5°. The numbers shown in the upper-right corner in each panel represent the annual and global averages of the difference in units of μg m^{-3}, and the numbers in brackets represent the annual and global averages of the relative difference in units of %.

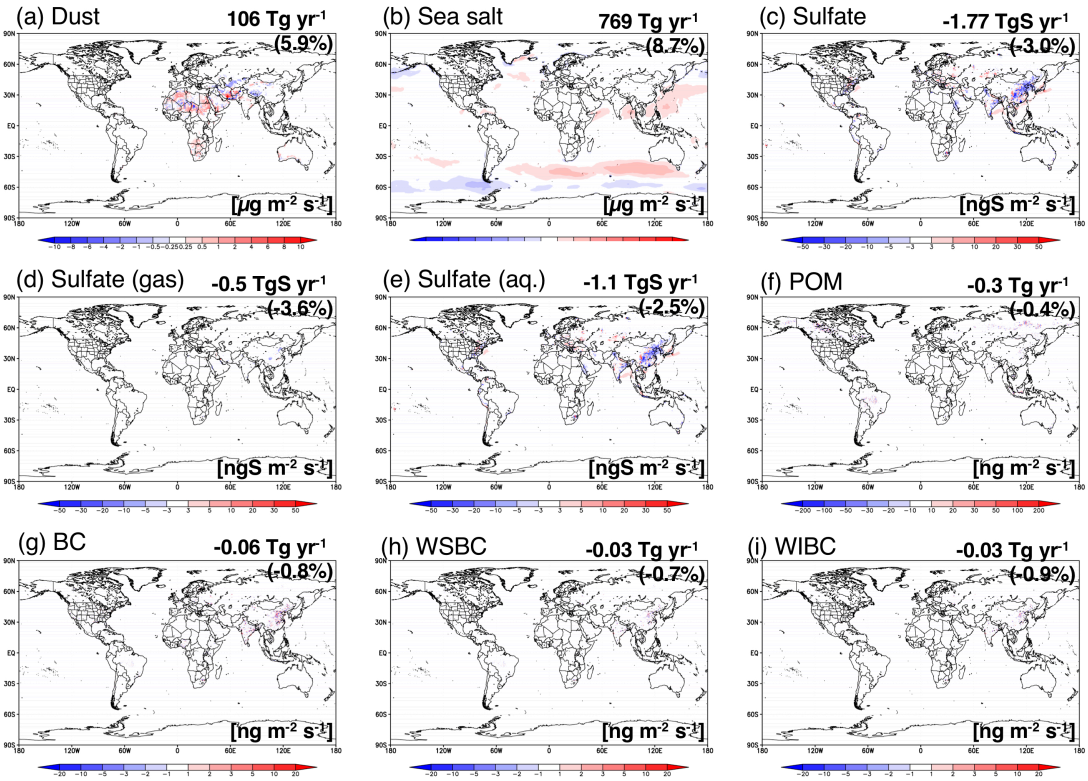

Figure S9: Global distributions of the differences in the emission fluxes for (a) dust, (b) sea salt, (c) total sulfate production, (d) sulfate production from gas-phase under the clear-sky, (e) sulfate production from aqueous-phase in clouds, (f) POM, (g) BC, (h) water-soluble BC (WSBC) and (i) water-insoluble BC (WIBC) between the HRM and LRM (LRM minus HRM) for the annual averages with a grid of 0.5°×0.5°. The numbers shown in the upper-right corner in each panel represent the annual and global averages of the difference in units of Tg yr^{-1} (TgS yr^{-1} only in (c) and (d)) and the numbers in brackets represent the annual and global averages of the relative difference in units of %.

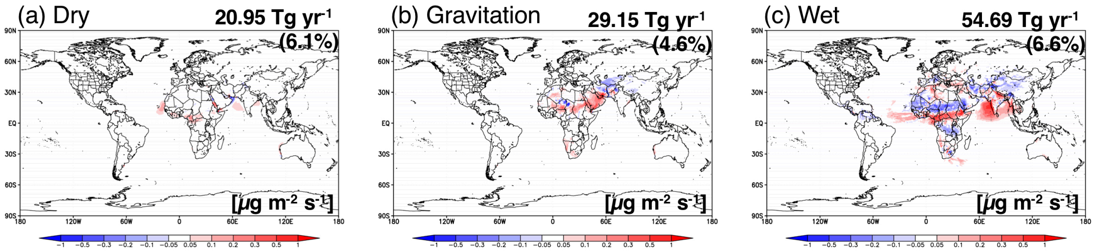

Figure S10: Global distributions of the differences in the fluxes for dust in (a) dry deposition, (b) gravitational deposition flux, and (c) wet deposition between the HRM and LRM (LRM minus HRM) for the annual averages with a grid of 0.5°×0.5°. The numbers shown in the upper-right corner in each panel represent the annual and global averages of the difference in units of Tg yr^{-1} and the numbers in brackets represent the annual and global averages of the relative difference in units of %.

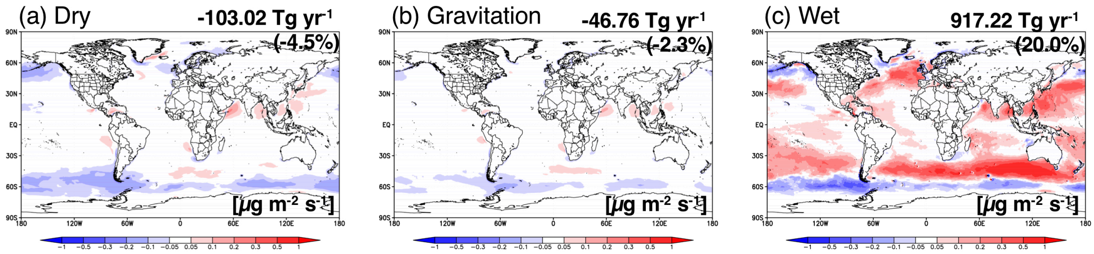

Figure S11: Same as Figure S10, but for the sea salt.

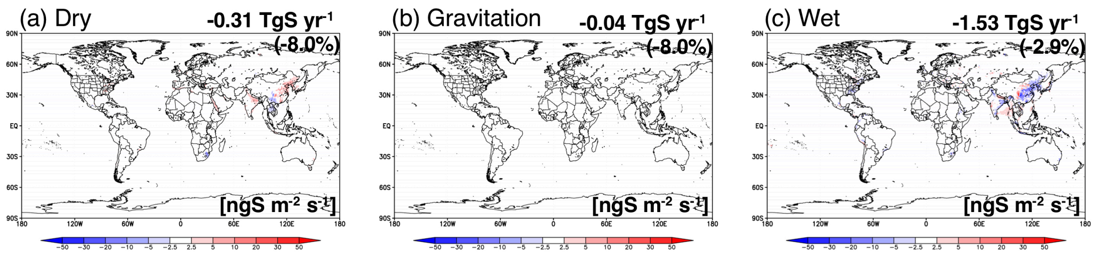

Figure S12: Same as Figure S10, but for the sulfate.

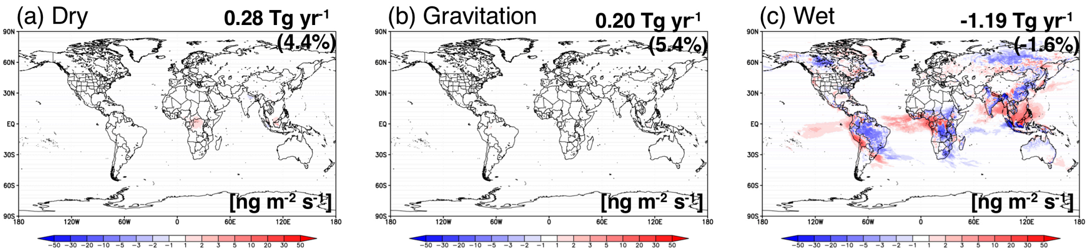

Figure S13: Same as Figure S10, but for the POM.

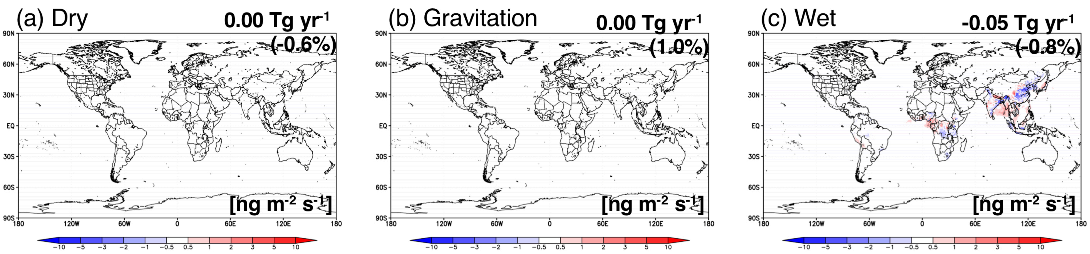

Figure S14: Same as Figure S10, but for the BC.

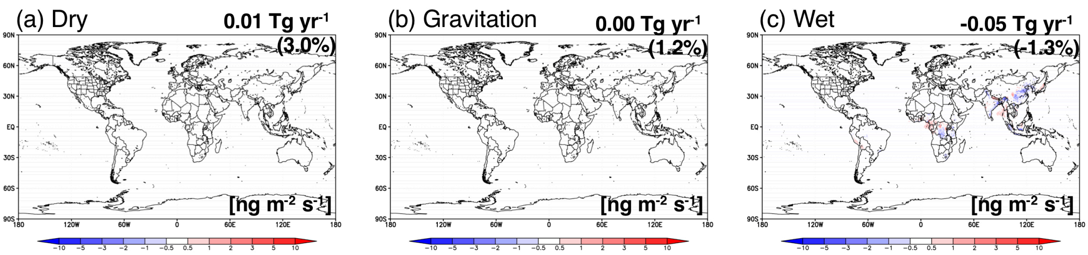

Figure S15: Same as Figure S10, but for the WSBC.

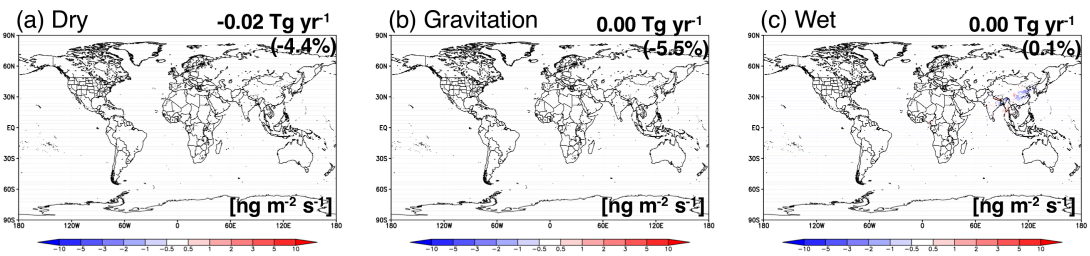

Figure S16: Same as Figure S10, but for the WIBC.